Journal of Medicinal Chemistry Article

J. Med. Chem. **2010,** *53,* 8309–8318 **8309**
DOI: 10.1021/jm101207e

Configuration of the 5′-Methyl Group Modulates the Biophysical and Biological Properties of Locked Nucleic Acid (LNA) Oligonucleotides

Punit P. Seth,*[,†] Charles R. Allerson,[†,∥] Andrew Siwkowski,[§] Guillermo Vasquez,[†] Andres Berdeja,[‡] Michael T. Migawa,[†] Hans Gaus,[‡] Thazha P. Prakash,[†] Balkrishen Bhat,[†,∥] and Eric E. Swayze[†]

[†]*Department of Medicinal Chemistry,* [‡]*Structural Biology, and* [§]*Antisense Drug Discovery, Isis Pharmaceuticals, Inc., 1891 Rutherford Road, Carlsbad, California 92011, United States.* [∥]*Current affiliation: Regulus Therapeutics.*

Received September 15, 2010

As part of a program aimed at exploring the structure− activity relationships of 2′,4′-bridged nucleic acid (BNA) containing antisense oligonucleotides (ASOs), we report the synthesis and biophysical and biological properties of *R*- and *S*-5′-Me LNA modified oligonucleotides. We show that introduction of a methyl group in the (*S*) configuration at the 5′-position is compatible with the high affinity recognition of complementary nucleic acids observed with LNA. In contrast, introduction of a methyl group in the (*R*) configuration reversed the stabilization effect of LNA. NMR studies indicated that the *R*-5′-Me group changes the orientation around torsion angle γ from the +sc to the ap range at the nucleoside level, and this may in part be responsible for the poor hybridization behavior exhibited by this modification. In animal experiments, *S*-5′-Me-LNA modified gapmer antisense olignucleotides showed slightly reduced potency relative to the sequence matched LNA ASOs while improving the therapeutic profile.

Introduction

Antisense olignucleotides (ASO[a]) bind to their cognate messenger RNA (mRNA) by Watson−Crick base pairing. Upon binding, they can modulate splicing, interfere with translation, or promote degradation of the mRNA via RNase H or RISC mediated mechanisms.[1] Unmodified oligonucleotides are unstable in biological media and are generally not suitable for therapeutic applications. A number of strategies including chemical modification of the sugar phosphate backbone[2] or formulation of the ASO using cationic lipids and other excipients[3,4] have been utilized for achieving pharmacological activity with oligonucleotides in animals. Second generation ASOs are among the most advanced oligonucleotides in the clinic.[5,6] These are chimeric oligonucleotides that are fully phosphorothioate (PS) modified and have a central "gap" of 8−16 2′-deoxyribose nucleotides flanked on the 3′- and the 5′-end with 2−5 2′-*O*-methoxyethyl (MOE) nucleotides. The PS modification improves stability of the oligonucleotide toward nuclease mediated degradation and also promotes binding to plasma proteins, thereby allowing ASO distribution into periphral tissues.[7,8] At the same time, the MOE nucleotides improve the binding affinity of the ASO for its cognate mRNA and also improve metabolic stability toward exonuclease digestion.[9−11]

To examine if further increases in affinity could benefit the therapeutic profile of second generation ASOs, we initiated a SAR program aimed at replacing MOE with other affinity enhancing nucleoside modifications such as 2′,4′-bridged nucleic acids (BNA).[12,13] Locked nucleic acid **1** (LNA, a representative member of the BNA class) modified ASOs have recently shown promising results for modulating gene expression via RNase H, splice correction, and miRNA based antisense mechanisms.[14−17] As part of our own SAR program,[18,19] we recently reported the synthesis and antisense properties of 2′,4′-constrained-2′*O*-alkyl (*R*-cEt **2**, *R*-cMOE **3**, *S*-cEt **4**, and *S*-cMOE **5**),[20,21] carbocyclic LNA (*R*-Me-cLNA **6**, *S*-Me-cLNA **7**, and methylene-cLNA **8**),[22,23] and other oxyamino BNA[24] modified oligonucleotides (Figure 1). We showed that introduction of methyl or methoxymethyl groups along the 2′,4′ bridging substituent did not adversely affect the hybridization properties relative to LNA. In contrast, the *R*- and *S*-Me-cLNA analogues **6** and **7**, where the 2′-oxygen atom of LNA is replaced with a substituted carbon atom, were less stabilizing in T_m studies. Interestingly, the methylene-cLNA **8** modification was found to be slightly more stabilizing as compared to LNA in T_m experiments, and this observation was rationalized by structural studies.[23] As an extension of the above SAR exercise, we wanted to evaluate the antisense properties of modifications **9** (*R*-5′-Me-LNA) and **10** (*S*-5′-Me-LNA) which have a methyl group at the 5′-position of the LNA sugar moeity.

As such, 5′-alkyl substituted nucleic acids have been reported in the literature (Figure 2). Saha and co-workers reported the synthesis and thermal denaturation studies of 5′-methyl-DNA.[25] They found that introduction of a methyl group (1:1 mixture of (*R*)- and (*S*)-isomers) at the 5′-position

*To whom correspondence should be addressed. Phone: 760-603-2587. Fax: 760-603-3891. E-mail: pseth@isisph.com.

[a] Abbreviations: BNA, 2′,4′-bridged nucleic acid; ASO, antisense oligonucleotide; LNA, locked nucleic acid; *R*-5′-Me-LNA, (*R*)-5′-methyl-locked nucleic acid; *S*-5′-Me-LNA, (*S*)-5′-methyl-locked nucleic acid; MOE, 2′-*O*-methoxyethyl RNA; cEt, 2′,4′-constrained-2′*O*-ethyl bridged nucleic acid; cMOE, 2′,4′-constrained-2′*O*-methoxyethyl bridged nucleic acid; cLNA, carba locked nucleic acid; CNA, constrained nucleic acid; Nap, 2-methylnaphthalene or naphthyl; DDQ, 2,3-dichloro-5,6-dicyano-*p*-benzoquinone; sc, synclinal; ap, antiperiplanar; PS, phosphorothioate; SVPD, snake venom phosphodiesterase; T_m, melting temperature; PTEN, phosphatase and tensin homologue.

Published on Web 11/08/2010

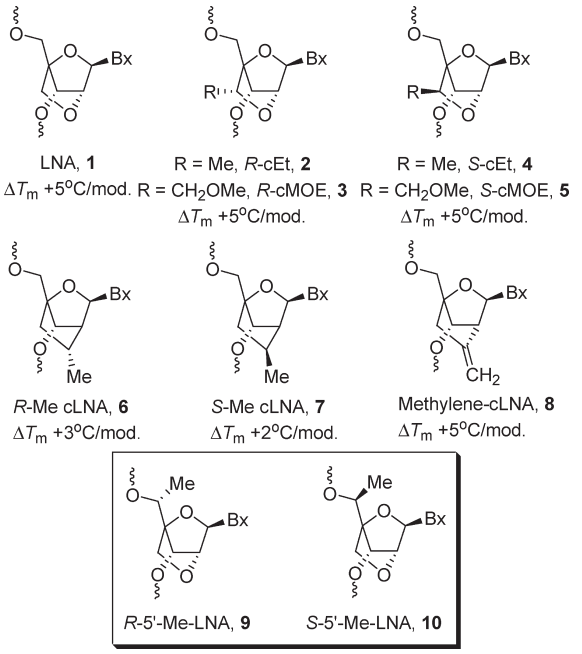

Figure 1. Structure and thermal stability properties of LNA, *R*- and *S*-cEt, *R*- and *S*-cMOE, *R*- and *S*-Me-cLNA, and vinyl-cLNA nucleic acid analogues.

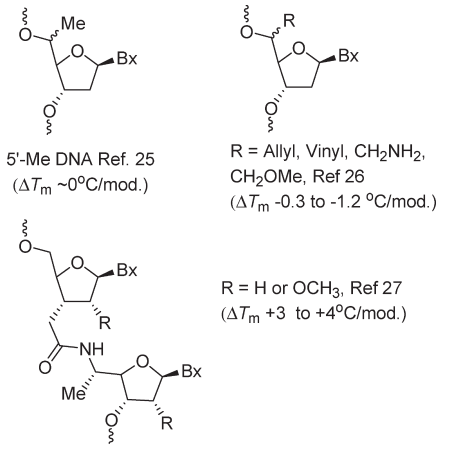

Figure 2. Hybridization properties of some 5′-alkyl nucleic acids reported in the literature.

of the furanose ring in DNA had a slight destabilizating effect on duplex stability (ΔT_m from 0 to −0.4 °C/mod.) while greatly increasing stability toward nuclease degradation. Later Wang reported the synthesis and thermal stability of (*S*)-5′-allyl, -vinyl, -aminomethyl, and -methoxymethyl substituted DNA.[26] They also observed a modest reduction in duplex stability (ΔT_m from −0.3 to −1.2 °C/mod.) for all the modifications evaluated. DeMesmaeker introduced a methyl group in either configuration at the 5′-position of C3′-CH_2-CONH-C5′amide linked DNA and 2′-*O*-Me RNA.[27] They saw improvements in thermal stability only when the methyl group was present in the (*S*) configuration (ΔT_m from +3 to +4 °C/mod.). They attributed the improved thermal stability to conformational preorganization of the amide bond upon introduction of the 5′-methyl group. In addition to the examples above, other 5′-alkyl substituted nucleic acids have also been described in the literature. Some notable examples include bi- and tricyclo DNA by Leumann,[28] α- and β-D-constrained nucleic acids

Scheme 1. Synthesis of *R*- and *S*-5′-Me-LNA Nucleosides

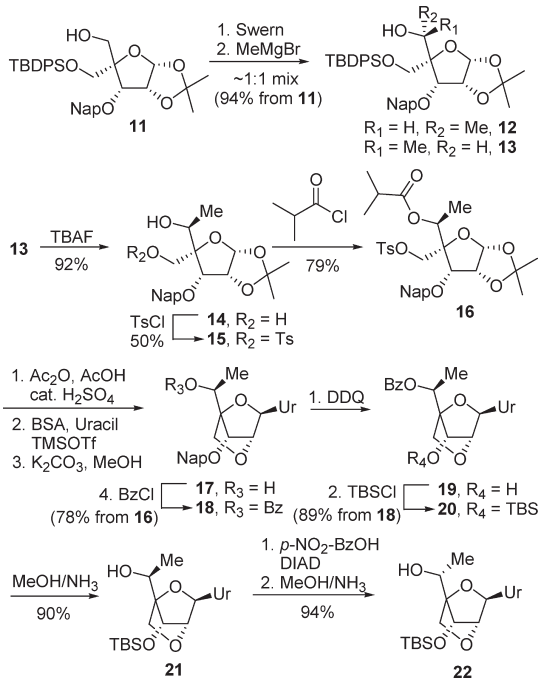

(CNA) by Escudier,[29,30] 5′-*C*- to 5′-*C*-alkyl linked cyclic dinucleotides by Nielsen,[31] and allofuranosylcytosine by Pitsch and co-workers.[32]

However, with the exception of the limited characterization of the biophysical properties of 5′-alkyl substituted nucleic acid analogues described above, there is little else known regarding the antisense properties of other oligonucleotide analogues which are substituted at the 5′-position of the furanose sugar moeity. In this report, we present the synthesis, biophysical, and biological characterization of *R*- and *S*-5′-Me-LNA modified oligonucleotides.

Results and Discussion

The synthesis of the *R*- and *S*-5′-methyl LNA nucleosides started from the known 3′-*O*-naphthylallofuranose derivative **11**[21] (Scheme 1). Oxidation of the hydroxyl group followed by addtion of MeMgBr resulted in the formation of a partially separable mixture of 5′-Me sugars **12** and **13**. Since we needed access to both the isomers for our intital evaluation, we did not attempt to improve the stereoselectivity of the organometallic addition at this stage. Treatment of **13** with TBAF provided diol **14** (95%). Selective tosylation of the primary alcohol in **14** provided **15** in moderate yield (50%). The major byproducts were an unseparable mixture of tosylate ester arising from tosylation of the secondary alcohol and the ditosyl sugar (25%), along with unreacted **13** (18%). Protection of the secondary 5′-hydroxyl group in **15** as the isobutyryl ester provided sugar **16**. Acetolysis of the 1,2-acetonide, followed by a Vorbruggen reaction with persilylated uracil, provided the crude nucleoside which was treated with potassium carbonate in methanol to provide the cyclized nucleoside **17**. While the 3′-*O*-Nap group could be deprotected at this stage, we were unable to selectively protect the secondary 5′-hydroxyl as the DMTr ether in the presence of the unprotected 3′-hydroxyl group. Moreover, we were unable to remove the naphthyl protecting group with DDQ or by hydrogenation in the presence of the 5′-*O*-DMTr protecting group. As a result, the secondary 5′-hydroxyl group was reprotected as the

Scheme 2. Synthesis of *R*- and *S*-5′-Me LNA Phosphoramidites

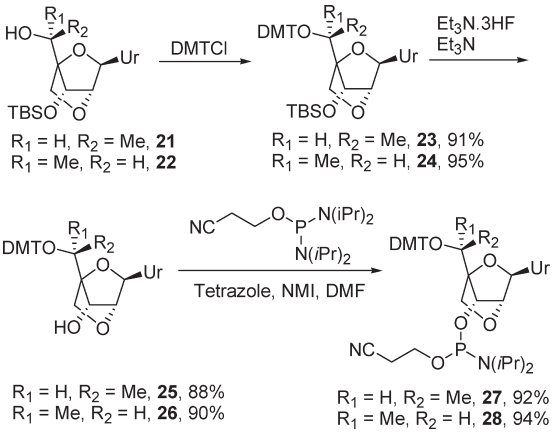

Scheme 3. Synthesis of a Crystalline Sugar Intermediate **29** for Confirmation of the Stereochemistry of the 5′-Me Substituent

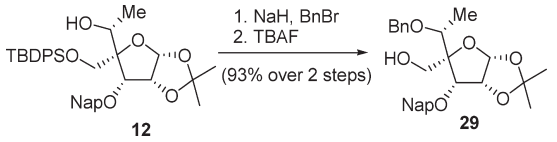

benzoyl ester to provide **18** (78%, over four steps). Removal of the naphthyl group with DDQ[21] provided nucleoside **19**. Reprotection of the 3′-hydroxyl as the TBS ether provided **20** (89% from **18**). Subsequent removal of the 5′-*O*-benzoyl group provided nucleoside **21** (90%). While the synthesis of the corresponding *R*-5′-Me-LNA nucleoside **22** could be accomplished starting from the sugar **13**, we were able to invert the 5′-hydoxyl group in **21** by means of a Mitsunobu reaction to provide nucleoside **22** after removal of the *p*-nitrobenzoyl group.

Preparation of the 5′-*O*-DMTr protected phosphoramidites from nucleosides **21** and **22** was accomplished in a straightforward manner (Scheme 2). Protection of the secondary hydroxyl groups in **21** and **22** using DMTrCl provided nucleosides **23** (91%) and **24** (95%), respectively. Removal of the 3′*O*-silyl protecting group in **23** and **24** using buffered triethylamine trihydrofluoride provide nucleosides **25** (88%) and **26** (90%), respectively. A phosphitylation reaction provided the desired phosphoramidites **27** (92%) and **28** (94%).

The stereochemistry of the 5′-methyl group in sugar intermediate **12** was unambigously assigned using X-ray crystallography (Scheme 3). Protection of the secondary 5′-hydroxyl group as the benzyl ether followed by removal of the TBDPS group provided a crystalline intermediate **29**. The stereochemistry of the 5′-methyl group in sugar intermediate **29** and thereby **12** was assigned as (*R*) by X-ray crystallography (Supporting Information). Thus, the stereochemistry of the 5′-methyl group in sugar intermediate **13** and therefore nucleoside **21** has to be (*S*).

The *R*-5′-Me-LNA **9** and *S*-5′-Me-LNA **10** modified oligonucleotides were prepared using standard phosphoramidite chemistry and evaluated in thermal stability experiments using protocols described previously.[21] We first evaluated the effect of these modifications on duplex thermal stability (T_m) using a sequence previously described by Imanishi[13] for the evaluation of LNA oligonucleotides (Table 1). In this sequence, the *S*-5′-Me-LNA (**A2**, ΔT_m = +4.6 °C/mod. vs RNA, ΔT_m = −2.2 °C/mod. vs DNA) modified oligomer showed comparable duplex thermal stability as LNA (**A4**, ΔT_m = +4.5 °C/mod. vs RNA; ΔT_m = +0.1 °C/mod. vs DNA) with RNA but not with DNA complements. In contrast, the *R*-5′-Me-LNA **A3** modification reduced duplex thermal stability with both RNA (−0.9 °C/mod.) and DNA (−4.8 °C/mod.) complements. To confirm the divergent hybridization behaviors of the *R*- and *S*-5′-Me-LNA isomers, we evaluated these modifications in a second sequence which has three incorporations of the modified nucleoside.[33] Once again, *S*-5′-Me-LNA (**B2**, ΔT_m = +5.6 °C/mod. vs RNA; ΔT_m = +2.3 °C/mod. vs DNA) showed LNA-like (**B4**, ΔT_m = +6.1 °C/mod. vs RNA; ΔT_m = +3.6 °C/mod. vs DNA) improvements in duplex thermal stability for RNA and DNA complements. Also consistent with our previous observation, *R*-5′-Me-LNA **B3** was less stabilizing (+2.6 °C/mod. vs RNA, −0.1 °C/mod. vs DNA) compared to the *S*-5′-Me-LNA modified oligonucleotide duplexes.

The differential thermal stability properties shown by the *R*-5′-Me-LNA and *S*-5′-Me-LNA modifications are perplexing and not easily explained. The improved thermal affinity for LNA oligonucleotides has been rationalized by a number of factors. Initially, it was proposed that the improved thermal affinity was a result of conformational preorganization, a consequence of locking the furanose ring in the C3′-endo conformation.[34] Subsequent studies with abasic LNA nucleotides and with seco-LNA nucleosides showed that no improvements in thermal affinities were observed in the absence of the nucleobase or with the seco-LNA derivatives. These authors concluded that the improvements in thermal affinity of LNA originate from improved intrastrand nucleobase stacking and not backbone preorganization alone.[35] Early NMR studies showed that introduction of LNA nucleosides into DNA cause conformational tuning of the adjacent sugar residues into the N-type conformation.[36,37] Further NMR studies of LNA modified DNA−RNA duplexes established that LNA-induced changes in electron density at the brim of the minor groove alters the pseudo-rotational profile of the 3′-flanking nucleotide toward an N-type conformation resulting in the formation of more stable A-type duplexes.[38] Recent studies using spectroscopic and calorimetric techniques showed that LNA results in increased enthalpy of hybridization that compensates for the unfavorable entropic changes and that formation of LNA modified duplex is accompanied by higher uptake of counterions and lower uptake of water.[39] This result corroborates earlier crystal structure data of a self-complementary LNA modified DNA decamer where no increase in the hydration of the LNA sugar residue relative to 2′-*O*-Me RNA was observed.[40] However, none of these arguments provided a rationale of why configuration of the 5′-methyl group has a divergent impact on the hybridization properties of *R*- and *S*-5′-Me-LNA modified oligonucleotides.

To examine the possibility that introduction of the 5′-Me group affects the rotational freedom around the C4′−C5′ bond in LNA, we carried out a conformational analysis of *R*- and *S*-5′-Me-LNA at the nucleoside level. It is well-known that restricted rotation exists around the C4′−C5′ bond in nucleosides with three possible lower energy conformations (Figure 3).[41] Of these, conformations **I** and **II**, which place the 4′- and the 5′-oxygen atoms in gauche orientation, are preferred for electronic reasons. Conformation **I** (torsion angle γ in +sc range) is further stabilized by a nonbonding interaction between H6 in pyrimidines (or H8 in purines) and the 5′-oxygen atom[42] and is the preferred conformation for hybridization found in both RNA and DNA duplexes. For *S*-5′-Me

Table 1. Thermal Stability Measurements of *S*-5′-Me-LNA, *R*-5′-Me-LNA, and LNA versus Complementary RNA and DNA[a]

oligomer	modification	sequence (5′−3′)	T_m (°C) vs RNA	ΔT_m (°C)/ mod.	T_m (°C) vs DNA	ΔT_m (°C)/ mod.	$(T_{mRNA} - T_{mDNA})$/ no. mod. (°C)
A1	DNA	d(GCGTTTTTTGCT)	45.6		50.9		
A2	*S*-5′-Me-LNA	d(GCGTT**U**TTTGCT)	50.2	+4.6	48.7	−2.2	+1.5
A3	*R*-5′-Me-LNA	d(GCGTT**U**TTTGCT)	44.7	−0.9	46.1	−4.8	−1.4
A4	LNA	d(GCGTT**U**TTTGCT)	50.1	+4.5	51.0	+0.1	−0.9
B1	DNA	d(CCAGTGATATGC)	42.6	0	48.7	0	0
B2	*S*-5′-Me-LNA	d(CCAG**U**GAUAUGC)	59.4	+5.6	57.9	+2.3	+0.5
B3	*R*-5′-Me-LNA	d(CCAG**U**GAUAUGC)	50.7	+2.6	50.8	+0.7	0
B4	LNA	d(CCAG**U**GAUAUGC)	61.0	+6.1	59.4	+3.6	+0.5

[a] Bold letter indicates modified residue. T_m values were measured in 10 mM sodium phosphate buffer (pH 7.2) containing 100 mM NaCl and 0.1 mM EDTA. Sequence of RNA complement 5′-r(AGCAAAAAACGC)-3′ and of DNA complement 5′-d(AGCAAAAAACGC)-3′ for oligonucleotides **A1**, **A2**, **A3** and **A4**. Sequence of RNA complement was 5′-r(GCAUAUCACUGG)-3′ and that of DNA complement was 5′-d(GCATATCACTGG)-3′ for oligonucleotides **B1**, **B2**, **B3**, and **B4**.

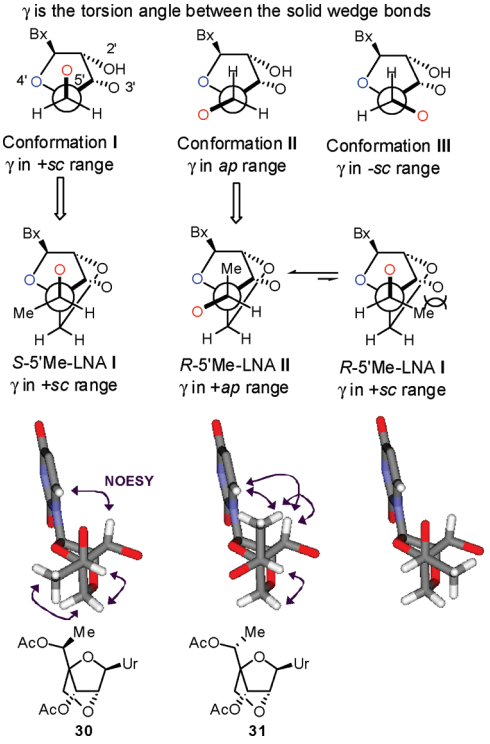

Figure 3. Structural analysis to rationalize conformation around the C4′−C5′ bond of (*S*)-5′-Me- and (*R*)-5′-Me-LNA. Double headed arrows denote relevant NOESY cross-peaks in **30** and **31**. Protecting groups on structural models not shown for clarity.

LNA **30**, conformation **I** is most likely the preferred conformation, as it places the methyl group in an orientation devoid of unfavorable steric interactions. In contrast, in *R*-5′-Me LNA nucleoside **31** the methyl group eclipses the 3′-hydroxyl in conformation **I**. It is possible that this nucleoside prefers conformation **II** (torsion angle γ in +ap range) which relieves the unfavorable eclipsing interaction. This hypothesis is supported by NMR data, where the H6 in the *S*-5′-Me nucleoside ($\delta \approx 7.9$ ppm) is consistently more downfield compared to the *R*-5′-Me isomer ($\delta \approx 7.5$ ppm), irrespective of the protecting group on the 5′-hydroxyl. Presumably, H6 is more deshielded by proximity to the 5′-oxygen in conformation **I** but not in conformation **II**. In addition, NOESY cross-peaks were observed between H6, 5′-Me group, and the 3′H in the case of the *R*-5′-Me nucleoside **31** but not for the *S*-5′-Me isomer **30**. For nucleoside **30**, NOESY cross-peaks were observed between the 5′-Me group and bridging methylene hydrogens. For nucleoside **31**, no cross-peaks were observed between the 5′-methyl group and the bridging methylene hydrogens.

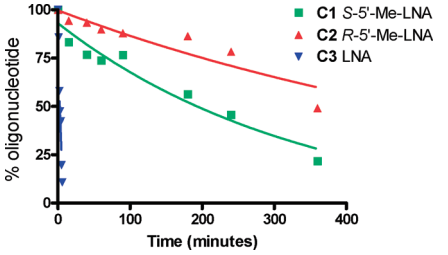

Figure 4. Nuclease stability of *S*-5′-Me-LNA, *R*-5′-Me-LNA, and LNA modified oligonucleotides. *R*- and *S*-5′-Me-LNA modified oligonucleotides show improved stability to SVPD compared to LNA. Sequence used for evaluation was TTTTTTTTTTUU. Upper case letters denote deoxynucleotide residues, while **UU** denote modified nucleosides. All internucleosidic linkages are phosphodiester. **C1** **UU** = *S*-5′-Me-LNA, **C2** **UU** = *R*-5′-Me-LNA, **C3** **UU** = LNA.

It is conceivable that the *R*-5′-Me- and *S*-5′-Me-LNA nucleosides exhibit the same conformational preferences around the C4′−C5′ bond in the oligonucleotide duplexes as those observed at the monomer level. This would suggest that the contribution of torsion angle γ (in the +sc range) to the improved stability of LNA duplexes is perhaps underappreciated and that γ in the +ap range is incompatible with the improved stability of A-form duplexes. However, γ in the +ap range has been observed in RNA duplexes and was associated with slightly improved interstrand nucleobase stacking.[43] In addition, other nucleoside modifications such as bicyclo DNA (bcDNA) and tricyclo DNA (tcDNA) position γ in the +ap range, albeit by a very different structural arrangement,[44,45] with tcDNA exhibiting improved thermal stability versus RNA. However, in the case of tcDNA the improved stability results from a compensatory change in two backbone torsion angles (β and γ).[46] At this point it is difficult to say if changes in other backbone torsions angles such as α and β occur in the case of *R*- and *S*-5′-Me-LNA modified oligonucleotides and if this has an impact on the overall thermal stability of the modified duplexes. This information can only be ascertained when high resolution NMR or crystal structures of modified oligonucleotide duplexes become available.

Oligonucleotides containing the *R*- and *S*-5′-Me-LNA modifications were next evaluated in nuclease stability experiments (Figure 4). 12-mer poly dT oligomers (**C1**−**C3**) with two modified residues at the 3′ end were digested with snake venom phosphodiesterase (SVPD). Significant increase in stability toward exonuclease digestion were observed for the

Table 2. Design, Sequence, and Thermal Stability Measurements of Gapmer ASOs Targeting Mouse PTEN

ASO	modification	sequence (5′−3′)[a]	mass calcd	mass obsd	% UV purity	T_m [b] (°C)
D1	*S*-5′-Me-LNA	**U**CATGGCTGCAG**CU**	4603.7	4603.2	95.5	61.5
D2	LNA	**T^{m}C**ATGGCTGCAG**^{m}CT**	4603.7	4602.8	96.3	64.0
E1	*S*-5′-Me-LNA	**CU**TAGCACTGGC**CU**	4563.7	4562.7	98.0	59.1
E2	LNA[c]	**^{m}CT**TAGCACTGGC**^{m}CT**	4563.7	4563.0	98.6	64.5
E3	*R*-5′-Me-LNA	**CU**TAGCACTGGC**CU**	4563.7	4562.8	96.3	51.6
F1	*S*-5′-Me-LNA	**CU**GCTAGCCTCTGGAT**UU**	5855.7	5855.2	95.6	61.0
F2	LNA	**^{m}CT**GCTAGCCTCTGGAT**TT**	5855.8	5854.8	94.3	61.6

[a] Bold letters indicate modified nucleosides in "wings" flanking a central DNA "gap" region. All internucleosidic linkages are phosphorothioate. T = thymine. U = uracil. A = adenine. G = guanine. C = cytosine. ^{m}C = 5-methylcytosine. [b] T_m values were measured in 10 mM sodium phosphate buffer (pH 7.2) containing 100 mM NaCl and 0.1 mM EDTA. Sequence of RNA complement for ASOs: **D1** and **D2**, 5′-(GGAAGCUGCAGCCAUGATGG)-3′; **E1** and **E2**, 5′-r(UCAAGGCCAGUGCUAAGAGU)-3′; **F1**and **F2**, 5′-r(UCAAAUCCAGAGGCUAGCAG)-3′. [c] LNA ASO **E2** with U/C monomers in the wings had a T_m of 61.3 °C. T_m of the sequence matched PS DNA ASO was 52.1 °C.

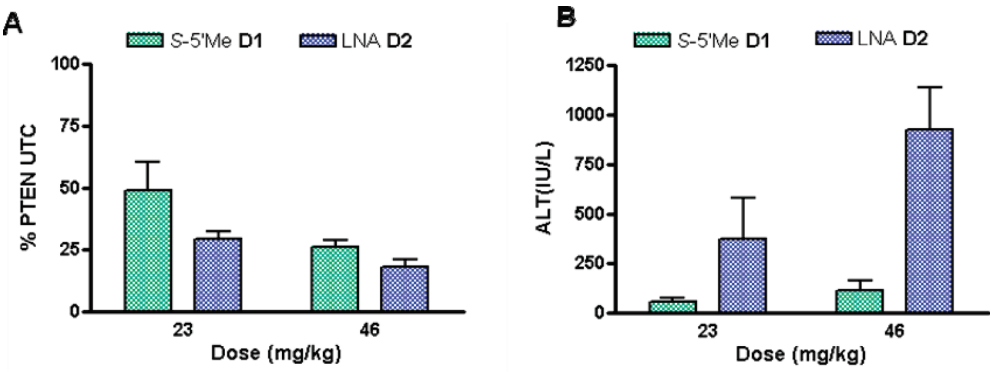

Figure 5. Mice (Balb-c, n = 4/group) were injected (ip) with a single dose of 23 and 46 mg/kg ASOs **D1** and **D2**: (A) % PTEN mRNA down-regulation in mouse liver versus saline treated animals; (B) plasma ALT (IU/L) levels after sacrifice.

R- and *S*-5′-Me-LNA modified oligonucleotides relative to LNA. The *R*-5′-Me-LNA oligomer **C1** exhibited the highest nuclease stability ($t_{1/2}$ = 8.1 h) compared to the *S*-5′-Me-LNA oligomer **C2** ($t_{1/2}$ = 3.5 h) and LNA **C3** ($t_{1/2}$ = 2.6 min). The improved stability observed with the *R*- and *S*-5′-Me-LNA modification could be a result of increased steric bulk around the phosphodiester backbone and/or distortions of the sugar phosphate backbone seen with this modification at the nucleoside level. Presumably, changes in either of these could interfere with the recognition of the oligonucleotide by the exonuclease.

Lastly, we evaluated the biological activity of *S*-5′-Me-LNA modified ASOs in animal experiments using three different oligonucleotide sequences (**D**, **E**, and **F**; Table 2) targeting mouse phosphatase and tensin homologue (PTEN) mRNA. All three sequences were fully phosphorothioate (PS) modified and had two modified nucleotides flanking the 3′- and 5′-ends of a 10-base (**D** and **E**) or a 14-base (**F**) deoxynucleotide gap. These sequences were described by us previously to evaluate the therapeutic profile of various 2′,4′-bridged nucleic acid (BNA) modified antisense oligonucleotides (ASOs).[20,23] We first evaluated these ASOs in thermal denaturation experiments with RNA complements where the *S*-5′-Me-LNA ASOs (**D1**, **E1**, and **F1**) generally exhibited similar thermal stability properties compared to the sequence matched LNA ASOs (**D2**, **E2**, and **F2**). The slightly higher T_m of LNA is most likely due to the presence of additional 5-methyl groups ($\Delta T_m \approx +0.5$ °C/mod.) on the pyrimidine nucleobases of the modified nucleotides.[47] We also evaluated the *R*-5′-Me-LNA modification in one sequence (**E3**), and it exhibited lower T_m compared to the sequence matched LNA (**E2**) and *S*-5′-Me-LNA (**E1**) ASOs. As a result, this modification was not further evaluated in any animal experiments.

In the first experiment, we evaluated the ability of the *S*-5′-Me-LNA modification to reduce the hepatotoxicity (as measured by plasma alanine amino transferase ALT levels) produced by a toxic LNA 14-mer ASO **D2** (Figure 5). Mice (n = 4/ group) were injected (ip) with a single dose of 23 and 46 mg/kg of the *S*-5′-Me-LNA ASO **D1** and LNA ASO **D2**, and animals were sacrificed 72 h after dosing. Liver PTEN mRNA was quantified using quantitative RT-PCR, and plasma ALT levels were measured. The *S*-5′-Me-ASO **D1** showed reduced potency for down-regulating PTEN mRNA in mouse liver at the 23 mg/kg dose, while both ASOs had roughly equivalent target knockdown at the 46 mg/kg dose. Elevations in ALT levels were observed for the LNA ASO **D2**, but not for *S*-5′-Me-LNA ASO **D1**, at both of the doses evaluated.

In a second experiment, we evaluated the effect of the *S*-5′-Me-LNA modification on the potency of an active 14-mer LNA ASO **E2** (Figure 6). Mice (n = 4) were injected twice a week for 3 weeks with 0.5, 1.5, 4.5, and 15 mg/kg *S*-5′-Me-LNA ASO **D1** and LNA ASO **D2**. Animals were sacrificed 72 h after the last dose, and liver PTEN mRNA levels were measured using quantitative RT-PCR. Plasma alanine transaminase (ALT) levels and organ weights were also recorded after sacrifice. For both ASOs, dose dependent reductions in liver PTEN mRNA levels were observed and the LNA ASO **D2** was more potent (ED_{50} = 3.1 mg/kg) compared to the *S*-5′-Me-LNA ASO **D1** (ED_{50} = 6.0 mg/kg). LNA ASO **D2** showed elevations in ALT levels for the high dose-group treated animals, while the *S*-5′-Me-LNA ASO did not show ALT increases relative to saline treated animals. Interestingly, the LNA ASO **D2** also showed increases in spleen weights (1.5 and 4.5 mg/kg dose) indicative of a proinflammatory effect, but no such increases were observed for the *S*-5′-Me-LNA

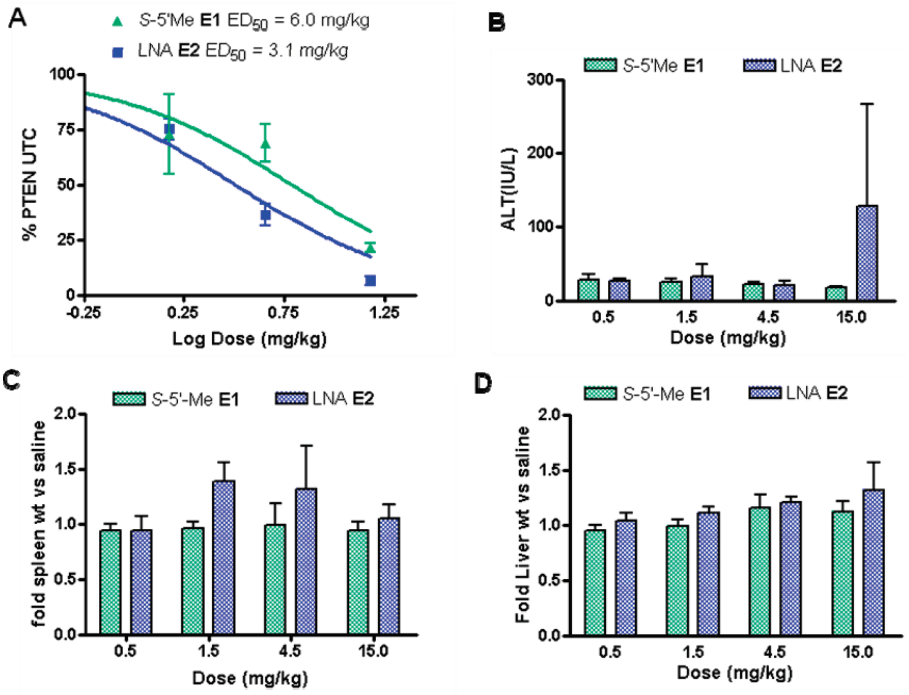

Figure 6. Mice (Balb-c, $n = 4$/group) were injected (ip) twice a week for 3 weeks with 0.5, 1.5, 4.5, and 15 mg/kg ASOs **E1** and **E2**: (A) % PTEN mRNA down-regulation in mouse liver versus saline treated animals; (B) plasma ALT (IU/L) levels after sacrifice; (C) fold increase in spleen weights versus saline treated group; (D) fold increase in liver weights versus saline treated group.

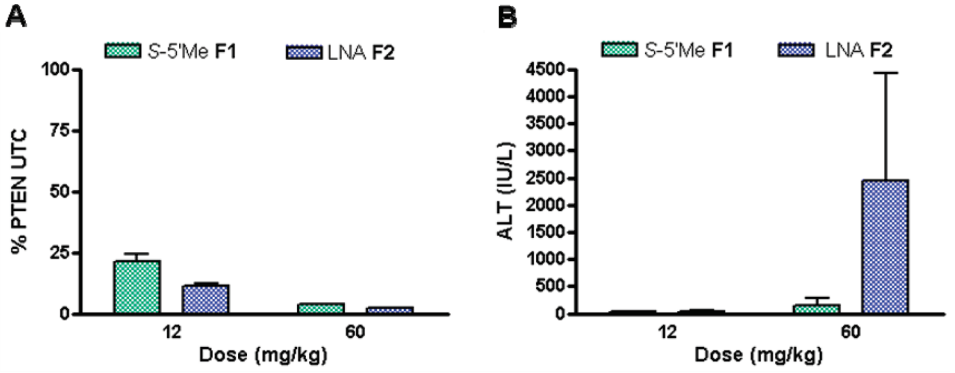

Figure 7. Mice (Balb-c, $n = 4$/group) were injected (ip) with a single dose of 12 and 60 mg/kg ASOs **F1** and **F2**: (A) % PTEN mRNA down-regulation in mouse liver versus saline treated animals; (B) plasma ALT (IU/L) levels after sacrifice.

ASO **D1**. The absence of spleen weight increase for the high dose (15 mg/kg) LNA ASO **D2** teated group is puzzling and could be related to other physiological changes unknown at this time. It is conceivable that the reduced proinflammatory profile for the *S*-5′-Me-LNA modified ASOs could be a result of increased bulk adjacent to the backbone phosphodiester linkage or due to slight distortions of the nucleic acid backbone caused by introduction of the 5′-Me group. Extrapolation of this data suggests that it might be possible to reduce the proinflammatory profile of nucleic acid drugs by introducing substitution at the 5′-position of an oligonucleotide.

In a third experiment, we evaluated the profile of the *S*-5′-Me-LNA modification in a 18-mer sequence targeting mouse PTEN. This sequence had a 14-mer deoxynucleotide gap flanked on the 3′- and 5′-ends with two modified nucleotides (Figure 7). Mice ($n = 4$/group) were injected ip with a single dose of 12 and 60 mg/kg *S*-5′-Me-LNA ASO **F1** and LNA ASO **F2**, and liver PTEN mRNA levels and plasma ALT levels were measured after sacrifice. The LNA ASO **F2** showed potent down-regulation (90%) of mouse PTEN mRNA in liver tissue at the lower dose, but hepatotoxicity was observed at the higher dose. In contrast, the *S*-5′-Me-LNA ASO **F1** also showed potent down-regulation of PTEN mRNA in mouse liver with only modest elevations in ALT levels at the high dose.

In conclusion, we report the synthesis, biophysical, and biological evaluation of *R*- and *S*-5′-Me-LNA modified oligonucleotides. While both these modification showed increased resistance toward exonuclease digestion, only the *S*-5′-Me-LNA modification showed similar hybridization properties as LNA. In contrast, the *R*-5′-Me-LNA reversed the stabilizing effect of LNA. NMR studies showed that introduction of the methyl group in the (*R*) configuration at the 5′-position of LNA nucleosides changes the orientation of torsion angle γ to the ap range instead of the preferred +sc range. These results suggest that in addition to locking the sugar conformation in the N-type sugar pucker and improved nucleobase stacking interactions, previously unknown sugar phosphate backbone torsional effects may be contributing to the improved thermal

stability of LNA modified oligonucleotide duplexes. Evaluation of the *S*-5′-Me-LNA modification in animal experiments suggested that this modification can reduce the hepatotoxicity and the proinflammatory profile of LNA ASOs. These data suggest that introduction of steric bulk or distortion of the phosphate backbone could be a general strategy to improve the nuclease resistance and reduce the proinflammatory effects of oligonucleotide drugs. However, additional experiments with multiple oligonucleotide sequences and motifs will have to be carried out to test the generality of this observation. Nonetheless, our data support further evaluation of the *S*-5′-Me LNA modification for diagnostic and therapeutic applications. Attempts to further understand the structural features responsible for the divergent biophysical and biological properties of 5′-Me substituted LNA oligonucleotides are in progress and will be reported in due course.

Experimental Section

All reagents were purchased from commercial vendors and used without any further purification. ^{1}H NMR spectra were obtained on a Bruker 300 MHz instrument. Low resolution mass spectrometry analyses were carried out on an Agilent 1100 series LCMS system equipped with a S.E.D.E.R.E. (France) Sedex 75 evaporative light scattering detector. Oligonucleotide synthesis, characterization, and T_m and nuclease stability meaurements were carried out as described previously.[18,20,24] Animal experiments and other in vivo analyses were carried out as described previously.[18,20,24] ED_{50} values and statistics were calculated using GraphPad Prism, version 4.00, for Windows (GraphPad Software, San Diego, CA, www.graphpad.com).

4-*C*-(*tert*-Butyldiphenylsilyloxy)-1,2-*O*-isopropylidene-(*S*)-5-*C*-methyl-3-*O*-(2-naphthyl)-α-D-ribofuranose (12) and 4-*C*-(*tert*-Butyldiphenylsilyloxy)-1,2-*O*-isopropylidene-(*R*)-5-*C*-methyl-3-*O*-(2-naphthyl)-α-D-ribofuranose (13). A solution of dimethylsulfoxide (14.9 mL, 210.0 mmol) in dichloromethane (20 mL) was added dropwise to a cold (−78 °C) solution of oxalyl chloride (9.12 mL, 105.0 mmol) in dichloromethane (400 mL). After the mixture was stirred for 45 min, a solution of alcohol **11** (50.0 g, 83.6 mmol) in dichloromethane (50 mL) was added to the mixture and the stirring was continued for another 1 h. Triethylamine (44.0 mL, 315.0 mmol) was added to the mixture, and the cooling bath was removed after 20 min. After being stirred for another 20 min, the mixture was carefully quenched with 5% HCl and the organic layer was washed with 5% HCl, saturated sodium bicarbonate, brine, dried (Na_2SO_4), and concentrated to provide the aldehyde which was used without any further purification.

MeMgBr (180 mL of a 1.4 M solution in THF) was added to a cold (−78 °C) suspension of cerium chloride (6.2 g, 25 mmol) in THF (250 mL). After the mixture was stirred for 30 min, a solution of the aldehyde from above in THF (100 mL) was added to the mixture via a cannula. The stirring was continued at −78 °C for another 5 h, and the mixture was warmed to 0 °C and stirred for 30 min. The reaction was then carefully quenched with 5% HCl, and the mixture was diluted with ethyl acetate. The organic layer was washed with 5% HCl, saturated sodium bicarbonate, brine, dried (Na_2SO_4), and concentrated. Purification by column chromatography (silica gel, eluting with 5−75% ethyl acetate in hexanes) provided **12** (16.1 g, 32%), a mixture of **12** and **13** (26.7 g, 52%), and **13** (5.0 g, 10%).

12. ^{1}H NMR (300 MHz, $CDCl_3$) δ: 7.85−7.66 (m, 8 H), 7.50−7.30 (m, 9 H), 5.76 (d, J = 4.0 Hz, 1 H), 4.84 (d, J = 12.1 Hz, 1H), 4.66 (d, J = 11.9 Hz, 1H), 4.55 (t, J = 4.5 Hz, 1H), 4.40 (m, 1 H), 4.28−4.18 (m, 2 H), 4.15 (d, J = 11.7 Hz, 1 H), 2.34 (br s, 1 H), 1.24 (s, 3 H), 1.21 (s, 3 H), 1.15 (d, J = 6.6 Hz, 3 H), 1.06 (s, 9 H). ^{13}C NMR (75 MHz, $CDCl_3$) δ: 136.0, 135.8, 135.2, 133.4, 133.3, 133.1, 133.0, 129.6, 129.5, 128.0, 127.9, 127.7, 127.7, 127.6, 126.4, 126.1, 125.9, 125.7, 113.0, 104.2, 90.3, 78.5, 77.1, 72.2, 67.8, 64.3, 26.9, 26.3, 25.9, 19.3, 16.1. ESI-MS $[M + Na]^+$ calcd 635.3; found 635.2.

13. ^{1}H NMR (300 MHz, $CDCl_3$) δ: 7.87−7.65 (m, 8 H), 7.54−7.27 (m, 9 H), 5.64 (d, J = 3.8 Hz, 1 H), 4.91 (d, J = 11.9 Hz, 1 H), 4.80 (d, J = 12.1 Hz, 1 H), 4.62−4.50 (m, 2 H), 4.25−4.09 (m, 2 H), 3.79 (d, J = 10.5 Hz, 1 H), 2.75 (d, J = 7.3 Hz, 1 H), 1.25 (s, 3 H), 1.23 (s, 3 H), 1.20 (d, J = 6.4 Hz, 3 H), 1.04 (s, 9 H). ^{13}C NMR (75 MHz, $CDCl_3$) δ: 135.8, 135.4, 133.2, 133.1, 132.8, 132.8, 129.7, 129.6, 128.1, 127.9, 127.7, 127.6, 126.9, 126.1, 126.0, 125.9, 113.2, 104.1, 87.6, 79.4, 78.1, 72.6, 70.8, 65.9, 26.9, 26.5, 26.1, 19.2, 17.6. ESI-MS $[M + Na]^+$ calcd 635.3; found 635.2.

4-*C*-(Hydroxymethyl)-1,2-*O*-isopropylidene-(*S*)-5-*C*-methyl-3-*O*-(2-naphthyl)-α-D-ribofuranose (14). Tetrabutylammonium fluoride (32 mL of a 1 M solution in THF) was added to a solution of **12** (16.1 g, 26.2 mmol) in THF (32 mL). After being stirred at room temperature for 16 h, the mixture was diluted with ethyl acetate and the organic layer was washed with water, brine, dried (Na_2SO_4), and concentrated. Purification by column chromatography (silica gel, eluting with 5−20% acetone in chloroform) provided **14** (9.0 g, 92%). ^{1}H NMR (300 MHz, $CDCl_3$) δ: 8.00−7.68 (m, 4 H), 7.61−7.34 (m, 3 H), 5.72 (d, J = 3.6 Hz, 1 H), 4.96 (d, J = 11.5 Hz, 1 H), 4.72 (d, J = 11.5 Hz, 1 H), 4.63 (dd, J = 4.0, 5.1 Hz, 1 H), 4.36 (d, J = 5.3 Hz, 1 H), 4.24 (d, J = 11.3 Hz, 1 H), 3.91 (br s, 1 H), 3.77 (m, 1 H), 2.67 (br s, 1 H), 2.18 (br s, 1 H), 1.65 (s, 3 H), 1.33 (s, 3 H), 1.24 (d, J = 6.4 Hz, 3 H). ^{13}C NMR (75 MHz, $CDCl_3$) δ: 134.6, 133.2, 128.5, 127.9, 127.7, 126.9, 126.3, 126.2, 125.6, 113.7, 104.7, 87.4, 79.4, 78.7, 72.8, 69.7, 63.4, 26.7, 26.0, 17.7. ESI-MS $[M + Na]^+$ calcd 397.2; found 397.1. HRMS (QTOF), calcd for $C_{21}H_{26}O_6Na$, 397.1627; found 397.1633.

1,2-*O*-Isopropylidene-(*S*)-5-*C*-methyl-3-*O*-(2-naphthyl)-4-*C*-(*p*-toluenesulfonyloxymethyl)-α-D-ribofuranose (15). *p*-Toluenesulfonyl chloride (9.7 g, 50.8 mmol) was added in portions (1.6 g every 1 h) to a cold (0 °C) solution of diol **14** (15.2 g, 40.7 mmol) in pyridine (80 mL). After the addition of tosyl chloride was complete, the mixture was warmed to room temperature and the stirring was continued for another 16 h after which the reaction was quenched by the addition of water. The mixture was diluted with ethyl acetate, and the organic layer was washed with water, 5% HCl, saturated sodium bicarbonate, brine, dried (Na_2SO_4), and concentrated. Purification by column chromatography (silica gel, eluting with 10−30% ethyl acetate in hexanes) provided **15** (10.4 g, 50%) along with a less polar unseparable mixture of the ditosyl and monotosyl isomers (9.02 g, 30%) and unreacted **14** (2.74 g, 18%). ^{1}H NMR (300 MHz, $CDCl_3$) δ: 7.90−7.80 (m, 4 H), 7.75 (d, J = 8.1 Hz, 2 H), 7.55−7.44 (m, 3 H), 7.21 (d, J = 8.3 Hz, 2 H), 5.63 (d, J = 3.6 Hz, 1 H), 4.86 (d, J = 12.1 Hz, 1 H), 4.75 (d, J = 12.1 Hz, 1 H), 4.64 (d, J = 10.0 Hz, 1 H), 4.53 (dd, J = 3.8, 5.1 Hz, 1 H), 4.33−4.23 (m, 2 H), 4.02 (br s, 1 H), 2.37 (s, 3 H), 1.94 (br s, 1 H), 1.38 (s, 3 H), 1.28 (s, 3 H), 1.16 (d, J = 6.4 Hz, 3 H). ^{13}C NMR (75 MHz, $CDCl_3$) δ: 144.7, 134.9, 133.2, 133.1, 132.6, 129.7, 128.2, 128.1, 128.0, 127.7, 126.8, 126.2, 126.1, 125.8, 113.7, 104.3, 86.4, 79.4, 77.3, 72.7, 69.1, 67.7, 26.6, 26.1, 21.6, 17.3. ESI-MS $[M + Na]^+$ calcd 551.2; found 551.1.

5-*O*-Isobutyryl-1,2-*O*-isopropylidene-(*S*)-5-*C*-methyl-3-*O*-(2-naphthyl)-4-*C*-(*p*-toluenesulfonyloxymethyl)-α-D-ribofuranose (16). Isobutyryl chloride (4.2 mL, 39.4 mmol) was added dropwise to a cold solution of **15** (10.4 g, 19.7 mmol), triethylamine (5.5 mL, 39.4 mmol), and dimethylaminopyridine (4.0 mmol, 0.49 g) in dichloromethane (40 mL). The mixture was gradually allowed to warm to room temperature and stirred for 5 h, after which it was diluted with dichloromethane and the organic layer was sequentially washed with 5% HCl, saturated sodium bicarbonate, brine (Na_2SO_4), dried, and concentrated. Purification by column chromatography (silica gel, eluting with 20−30% ethyl acetate in hexanes) provided **16** (9.2 g, 79%). ^{1}H NMR (300 MHz, $CDCl_3$) δ: 7.88−7.81 (m, 3 H), 7.80−7.73 (m, 3 H), 7.55−7.43 (m, 3 H), 7.30−7.20 (m, 2 H), 5.65 (d, J = 3.6 Hz, 1 H), 5.15

(q, J = 6.3 Hz, 1 H), 4.84 (d, J = 11.9 Hz, 1 H), 4.73 (d, J = 12.1 Hz, 1 H), 4.59−4.47 (m, 2 H), 4.33 (d, J = 10.0 Hz, 1 H), 4.04 (d, J = 5.1 Hz, 1 H), 2.43 (s, 3 H), 2.43−2.36 (m, 1H), 1.44 (s, 3 H), 1.31 (s, 3 H), 1.13 (d, J = 6.4 Hz, 3 H), 1.01 (d, J = 7.0 Hz, 3 H), 0.97 (d, J = 7.0 Hz, 3 H). ^{13}C NMR (75 MHz, $CDCl_3$) δ: 175.4, 144.6, 134.6, 133.2, 132.8, 129.7, 128.4, 128.1, 127.9, 127.7, 126.9, 126.3, 126.2, 125.6, 114.1, 104.3, 85.4, 79.4, 77.2, 72.7, 69.9, 68.1, 34.0, 26.7, 26.3, 21.6, 18.7, 18.7, 13.9. ESI-MS $[M + Na]^+$ calcd 621.2; found 621.1. HRMS (QTOF) calcd for $C_{32}H_{38}O_9SNa$, 621.2134; found 621.2138.

(1*R*,3*R*,4*R*,7*S*)-1-[1-(*S*)-(Benzoyloxy)ethyl]-7-(2-naphthyloxy)-3-(uracil-1-yl)-2,5-dioxabicyclo[2.2.1]heptane (18). Sulfuric acid (6 drops) was added to a solution of **16** (3.0 g, 5.0 mmol) and acetic anhydride (4.0 mL) in acetic acid (15 mL). After the mixture was stirred at room temperature for 1 h, the solvent was removed under reduced pressure on a rotary evaporator at room temperature. The oil was diluted with ethyl acetate and the organic layer was carefully washed with water, saturated sodium bicarbonate (until pH > 10), brine, dried (Na_2SO_4), and concentrated to provide a mixture of anomeric diacetates. The resulting foam was dried under reduced pressure for 16 h and used without any further purification.

N,*O*-Bis-trimethylsilylamide (6.2 mL, 25.0 mmol) was added to a suspension of the crude diacetate from above and uracil (1.1 g, 10.0 mmol) in acetonitrile (25 mL). The mixture was warmed until dissolution occurred and then cooled in an ice bath. TMSOTf (1.4 mL, 7.5 mmol) was added dropwise to the mixture, which was then transferred to an oil bath and refluxed for 2 h. The mixture was then cooled to room temperature, carefully quenched with half-saturated sodium bicarbonate solution, and diluted with ethyl acetate. The organic layer was washed with half-saturated sodium bicarbonate, brine, dried (Na_2SO_4), and concentrated to provide the crude nucleoside which was used without any further purification.

Potassium carbonate (2.0 g, 15.0 mmol) was added to a solution of the crude nucleoside from above in methanol (50 mL). After the mixture was stirred at room temperature for 16 h, the solid was collected by filtration and partitioned between ethyl acetate and water. The organic layer was further washed with water, brine, dried (Na_2SO_4), and concentrated to provide the cyclized nucleoside which was dried under reduced pressure for 16 h and used without any further purification.

Benzoyl chloride (0.75 mL, 6.5 mmol) was added to a cold (0 °C) solution of the cyclized nucleoside from above in pyridine (10 mL). After the mixture was stirred for 1 h in the ice bath, the reaction was quenched with methanol and diluted with ethyl acetate. The organic layer was washed with water, brine, dried (Na_2SO_4), and concentrated. Purification by column chromatography (silica gel, eluting with 0−20% acetone in dichloromethane) provided **18** (2.0 g, 78% from **16**). ^{1}H NMR (300 MHz, $CDCl_3$) δ: 8.77 (s, 1 H), 7.87−7.79 (m, 2 H), 7.73−7.51 (m, 6 H), 7.47−7.28 (m, 5 H), 5.68 (s, 1 H), 5.63 (q, J = 6.7 Hz, 1 H), 5.43 (d, J = 8.3 Hz, 1 H), 4.78 (d, J = 11.7 Hz, 1 H), 4.64−4.55 (m, 2 H), 4.18 (d, J = 7.7 Hz, 1 H), 3.91 (d, J = 7.7 Hz, 1 H), 3.74 (s, 1 H), 1.47 (d, J = 6.6 Hz, 3 H). ^{13}C NMR (75 MHz, $CDCl_3$) δ: 165.0, 162.8, 149.4, 138.5, 133.5, 133.5, 133.0, 132.9, 129.6, 129.2, 128.6, 128.6, 127.7, 127.7, 127.2, 126.4, 126.3, 125.5, 101.5, 88.9, 87.4, 76.5, 75.4, 72.4, 72.1, 65.8, 16.0. ESI-MS $[M + Na]^+$ calcd 515.1; found 515.1. HRMS (QTOF) calcd for $C_{29}H_{27}N_2O_7$, 515.1818; found 515.1815.

(1*R*,3*R*,4*R*,7*S*)-1-[1-(*S*)-(Benzoyloxy)ethyl]-7-(*tert*-butyldimethylsilyloxy)-3-(uracil-1-yl)-2,5-dioxabicyclo[2.2.1]heptane (20). 2,3-Dichloro-5,6-dicyano-*p*-benzoquinone (1.1 g, 5.0 mmol) was added to a biphasic solution of **18** (1.7 g, 3.3 mmol) in dichloromethane (33 mL) and water (2 mL). After the mixture was stirred at room temperature for 16 h, the solvent was removed and the residue was redissolved in ethyl acetate. The organic layer was washed with water, 10% sodium bisulfite, saturated sodium bicarbonate, brine, dried (Na_2SO_4), and concentrated. Purification by chromatography (silica gel, eluting with 20−35% acetone in dichloromethane) provided **19** (1.2 g, 98%) partially contaminated with DDQ byproduct. ^{1}H NMR (300 MHz, CDCl3) δ: 9.29 (br s, 1 H), 8.11−8.01 (m, 2 H), 7.72−7.45 (m, 4 H), 5.61 (s, 1 H), 5.54 (q, J = 6.7 Hz, 1 H), 5.33 (d, J = 8.1 Hz, 1 H), 4.45 (s, 1 H), 4.12 (d, J = 7.9 Hz, 1 H), 3.83 (d, J = 7.9 Hz, 1 H), 3.77 (s, 1 H), 3.68 (br s, 1 H), 1.51 (d, J = 6.6 Hz, 3 H). ESI-MS $[M + H]^+$ calcd 375.1; found 375.1.

tert-Butyldimethylsilyl chloride (1.5 g, 10.0 mmol) was added to a solution of **18** (1.2 g, 3.3 mmol) and imidazole (1.4 g, 20.0 mmol) in dimethylformamide (10 mL). After being stirred at room temperature for 38 h, the mixture was diluted with ethyl acetate and the organic layer was washed with water, brine, dried (Na_2SO_4), and concentrated. Purification by column chromatography (silica gel, eluting with 10−40% ethyl acetate in hexanes) provided **20** (1.5 g, 89%). ^{1}H NMR (300 MHz, $CDCl_3$) δ: 9.49 (s, 1 H), 8.00 (dd, J = 0.8, 8.4 Hz, 2 H), 7.92 (d, J = 8.1 Hz, 1 H), 7.69−7.59 (m, 1 H), 7.56−7.44 (m, 2 H), 5.72−5.65 (m, 2 H), 5.52 (m, 1 H), 4.34 (s, 1 H), 4.09 (d, J = 7.5 Hz, 1 H), 3.95 (s, 1 H), 3.86 (d, J = 7.5 Hz, 1 H), 1.48 (d, J = 6.6 Hz, 3 H), 0.83 (s, 9 H), 0.02 (s, 3 H), −0.08 (s, 3 H). ^{13}C NMR (75 MHz, $CDCl_3$) δ: 165.1, 163.5, 149.6, 138.7, 133.6, 129.9, 129.2, 128.7, 101.7, 89.5, 87.3, 79.0, 71.7, 70.8, 65.8, 25.4, 17.8, 16.1, −4.9, −5.3. ESI-MS $[M + H]^+$ calcd 489.2; found 489.2. HRMS (QTOF) calcd for $C_{24}H_{33}N_2O_7Si$, 489.2057; found 489.2069.

(1*R*,3*R*,4*R*,7*S*)-7-(*tert*-Butyldimethylsilyloxy)-1-[1-(*S*)-hydroxyethyl]-3-(uracil-1-yl)-2,5-dioxabicyclo[2.2.1]heptane (21). A solution of **20** (1.4 g, 2.9 mmol) in methanolic ammonia (30 mL, 7 N) was heated in a sealed vessel at 50 °C for 5 days, after which it was concentrated and purified by column chromatography (silica gel, eluting with 5−25% acetone in dichloromethane) to provide **21** (1.0 g, 90%) plus unreacted **20** (0.1 g, 7%). ^{1}H NMR (300 MHz, MeOD) δ: 7.87 (d, J = 8.1 Hz, 1 H), 5.59 (d, J = 8.3 Hz, 1 H), 5.44 (s, 1 H), 4.10 (s, 1 H), 4.03 (s, 1 H), 3.89 (m, 1 H), 3.80 (d, J = 7.7 Hz, 1 H), 3.58 (d, J = 7.7 Hz, 1 H), 1.15 (d, J = 6.6 Hz, 3 H), 0.82−0.75 (m, 9 H), 0.02 (s, 3 H), −0.02 (s, 3 H). ^{13}C NMR (75 MHz, MeOD) δ: 165.0, 150.5, 140.0, 100.7, 90.7, 87.2, 79.3, 71.4, 70.8, 61.8, 24.8, 17.9, 17.6, −6.1, −6.2. ESI-MS $[M + H]^+$ calcd 385.2; found 385.2.

(1*R*,3*R*,4*R*,7*S*)-7-(*tert*-Butyldimethylsilyloxy)-1-[1-(*R*)-hydroxyethyl]-3-(uracil-1-yl)-2,5-dioxabicyclo[2.2.1]heptane (22). Diisopropyl azodicarboxylate (0.51 mL, 2.6 mmol) was added to a cold (0 °C) solution of **21** (0.2 g, 0.5 mmol), triphenylphosphine (0.68 g, 2.6 mmol), and *p*-nitrobenzoic acid (0.43 g, 2.6 mmol) in THF (5 mL). After being stirred at room temperature for 16 h, the mixture was diluted with ethyl acetate and the organic layer was washed with water, brine, dried (Na_2SO_4), and concentrated. Purification by column chromatgraphy (silica gel, eluting with 50% ethyl acetate−hexane) provided the nitrobenzoyl ester contaminated with DIAD byproducts. To this mixture was added methanolic ammonia (8 mL of a 7 N solution), and the container was sealed and aged at room temperature for 16 h. The solvent was evaporated under reduced pressure and the residue was purified by column chromatography (silica gel, eluting with 0−30% acetone in dichloromethane) to provide **22** (0.19 g, 94% from **21**). ^{1}H NMR (300 MHz, MeOD) δ: 7.69 (d, J = 8.1 Hz, 1 H), 5.62 (d, J = 8.1 Hz, 1 H), 5.42 (s, 1 H), 4.18 (s, 1 H), 4.08−3.97 (m, 2 H), 3.93 (s, 1 H), 3.77 (d, J = 7.9 Hz, 1 H), 1.25 (d, J = 6.8 Hz, 3 H), 0.83−0.74 (m, 9 H), 0.00 (s, 3 H), −0.01 (s, 3 H). ^{13}C NMR (75 MHz, MeOD) δ: 166.1, 151.7, 140.9, 102.3, 91.8, 88.8, 81.2, 73.7, 72.9, 65.3, 26.1, 18.8, 18.8, −4.6, −4.9. ESI-MS $[M + H]^+$ calcd 385.2; found 385.1. HRMS (QTOF) calcd for $C_{17}H_{29}N_2O_6Si$, 385.1795; found 385.1802.

General Procedure for Preparing 5′-*O*-Dimethoxytrityl Protected Nucleosides. A mixture of nucleoside (1 equiv), 4,4′-dimethoxytrityl chloride (3 equiv), and 2,6-lutidine (3 equiv) in pyridine (0.3 M) was heated at 45 °C for 3 days. The reaction was quenched with methanol. The mixture was diluted with ethyl acetate, and the organic layer was washed with water, brine, dried (Na_2SO_4), and concentrated. Purification by column chromatography (silica gel, eluting with 30−40% ethyl acetate in hexanes) provided the 5′-*O*-DMT protected nucleoside.

(1*R*,3*R*,4*R*,7*S*)-7-(*tert*-Butyldimethylsilyloxy)-1-[1-(*S*)-(4,4′-dimethoxytrityloxy)ethyl]-3-(uracil-1-yl)-2,5-dioxabicyclo[2.2.1]heptane (23). 23 was prepared according to the general procedure using **21** (0.5 g, 1.3 mmol) to provide **23** (0.82 g, 91%). ^{1}H NMR (300 MHz, $CDCl_3$) δ: 9.19 (br s, 1 H), 8.10 (d, J = 8.1 Hz, 1 H), 7.50−7.18 (m, 9 H), 6.89−6.75 (m, 4 H), 5.74−5.63 (m, 2 H), 4.34 (s, 1 H), 4.25 (s, 1 H), 3.86 (d, J = 7.5 Hz, 1 H), 3.80 (d, J = 2.1 Hz, 6 H), 3.72 (dd, J = 7.1, 9.9 Hz, 2 H), 0.96 (d, J = 6.4 Hz, 3 H), 0.77 (s, 9 H), 0.04 (s, 3 H), −0.10 (s, 3 H). ^{13}C NMR (75 MHz, $CDCl_3$) δ: 163.4, 158.7, 149.7, 146.2, 139.5, 136.4, 136.3, 130.5, 128.3, 127.7, 127.0, 120.1, 113.0, 101.6, 91.8, 87.2, 86.4, 79.1, 72.0, 71.0, 66.1, 55.2, 25.5, 17.9, 17.8, −4.4, −4.9. ESI-MS $[M + Na]^+$ calcd 709.3; found 709.2. HRMS (QTOF) calcd for $C_{38}H_{46}N_2O_8SiNa$, 709.2921; found 709.2912.

(1*R*,3*R*,4*R*,7*S*)-7-[*tert*-Butyldimethylsilyloxy]-1-[1-(*R*)-(4,4′-dimethoxytrityloxyethyl]-3-(uracil-1-yl)-2,5-dioxabicyclo[2.2.1]heptane (24). 24 was prepared according to the general procedure using **22** (0.19 g, 0.5 mmol) to provide **24** (0.27 g, 95%). ^{1}H NMR (300 MHz, $CDCl_3$) δ: 8.42−8.31 (m, 1 H), 7.60 (d, J = 8.3 Hz, 1 H), 7.52−7.44 (m, 2 H), 7.43−7.14 (m, 7 H), 6.81 (d, J = 8.9 Hz, 4 H), 5.61 (s, 1 H), 5.59−5.52 (m, 1 H), 4.24 (s, 1 H), 3.96 (d, J = 7.9 Hz, 1 H), 3.84 (s, 1 H), 3.78 (s, 6 H), 3.69 (d, J = 8.1 Hz, 1 H), 3.58 (m, 1 H), 1.11 (d, J = 6.6 Hz, 3 H), 0.78 (s, 9 H), 0.00 (s, 3 H), −0.02 (s, 3 H). ^{13}C NMR (75 MHz, $CDCl_3$) δ: 162.7, 158.6, 149.4, 146.3, 138.8, 136.3, 136.2, 130.3, 130.3, 127.9, 127.8, 126.8, 113.1, 113.1, 101.8, 91.5, 87.7, 86.7, 79.5, 73.3, 71.8, 67.1, 55.2, 25.5, 17.8, 17.5, −4.7, −5.1. ESI-MS $[M + Na]^+$ calcd 709.3; found 709.2.

General Procedure for Deprotecting 3′*O*-TBDMS Group. A solution of tetrabutylammonium fluoride (1.2 equiv, 1 M in THF) was added to a solution of nucleoside (1 equiv) in THF (0.3 M). After being stirred at room temperature for 16 h, the mixture was diluted with ethyl acetate and the organic layer was washed with water, brine, dried (Na_2SO_4), and concentrated. Purification by column chromatography (silica gel, eluting with 30−40% acetone in dichloromethane) provided the 3′-deprotected nucleoside.

(1*R*,3*R*,4*R*,7*S*)-1-[1-(*S*)-(4,4′-Dimethoxytrityloxy)ethyl]-7-hydroxy-3-(uracil-1-yl)-2,5-dioxabicyclo[2.2.1]heptane (25). 25 was prepared according to the general procedure using **23** (0.2 g, 0.29 mmol) to provide **25** (0.15 g, 88%). ^{1}H NMR (300 MHz, $CDCl_3$) δ: 9.72 (br s, 1 H), 8.00 (d, J = 8.1 Hz, 1 H), 7.54−7.34 (m, 6 H), 7.33−7.15 (m, 3 H), 6.84 (dd, J = 1.2, 8.8 Hz, 4 H), 5.66 (d, J = 8.1 Hz, 1 H), 5.60 (s, 1 H), 4.36 (s, 1 H), 4.01 (d, J = 4.5 Hz, 1 H), 3.83−3.73 (m, 2 H), 3.80 (s, 6H), 3.65 (d, J = 7.9 Hz, 1 H), 2.45 (d, J = 4.9 Hz, 1 H), 1.04 (d, J = 6.4 Hz, 3 H). ^{13}C NMR (75 MHz, $CDCl_3$) δ: 163.9, 158.7, 158.7, 149.9, 145.9, 139.5, 136.2, 136.1, 130.6, 128.3, 127.8, 127.0, 113.1, 113.1, 101.6, 91.3, 87.0, 86.8, 79.3, 71.6, 70.3, 65.4, 55.3, 55.2, 18.2. ESI-MS $[M + Na]^+$ calcd 595.2; found 595.2.

(1*R*,3*R*,4*R*,7*S*)-1-[1-(*R*)-(4,4′-Dimethoxytrityloxy)ethyl]-7-hydroxy-3-(uracil-1-yl)-2,5-dioxabicyclo[2.2.1]heptane (26). 26 was prepared according to the general procedure, using **24** (0.26 g, 0.4 mmol) to provide **26** (0.20 g, 90%). ^{1}H NMR (300 MHz, $CDCl_3$) δ: 9.05−8.91 (m, 1 H), 7.52−7.46 (m, 2 H), 7.45−7.35 (m, 4 H), 7.32−7.16 (m, 4 H), 6.88−6.80 (m, 4 H), 5.57 (s, 1 H), 5.53 (d, J = 8.1 Hz, 1 H), 4.35 (s, 1 H), 3.99 (q, J = 8.5 Hz, 2 H), 3.79 (s, 6 H), 3.78−3.69 (m, 2 H), 2.94 (br s, 1 H), 1.17 (d, J = 6.6 Hz, 3 H). ^{13}C NMR (75 MHz, $CDCl_3$) δ: 163.1, 158.8, 158.7, 149.6, 145.8, 138.6, 136.0, 135.8, 130.3, 130.3, 128.0, 127.9, 127.0, 113.3, 113.2, 101.7, 89.8, 87.4, 86.9, 79.8, 71.9, 71.5, 67.9, 55.3, 18.2. ESI-MS $[M + Na]^+$ calcd 595.2; found 595.2. HRMS (QTOF) calcd for $C_{32}H_{32}N_2O_8Na$, 595.2056; found 595.2055.

General Procedure for Preparation of Nucleoside Phosphoramidites. 2-Cyanoethyl *N*,*N*′-tetraisopropylphosphoramidite (1.5 equiv) was added to a solution of nucleoside (1 equiv), tetrazole (0.8 equiv), and *N*-methylimidazole (0.25 equiv) in DMF (0.2 M). After being stirred for 8 h at room temperature, the mixture was poured into EtOAc and the organic phase was washed with brine, dried (Na_2SO_4), and concentrated. Purification by column chromatography (silica gel, eluting with 50−60% ethyl acetate in hexanes) provided the desired nucleoside phosphoramidite.

(1*R*,3*R*,4*R*,7*S*)-7-[2-Cyanoethoxy(diisopropylamino)phosphinoxy]-1-[1-(*S*)-(4,4′-dimethoxytrityloxy)ethyl]-3-(uracil-1-yl)-2,5-dioxabicyclo[2.2.1]heptane (27). 27 was prepared according to the general procedure using **24** (0.14 g, 0.24 mmol) to provide **27** (0.16 g, 87%). ^{31}P NMR (121 MHz, $CDCl_3$) δ: 149.1, 148.5. HRMS (QTOF) calcd for $C_{41}H_{48}N_4O_9P$, 771.3159; found 771.3180.

(1*R*,3*R*,4*R*,7*S*)-7-[2-Cyanoethoxy(diisopropylamino)phosphinoxy]-1-[1-(*R*)-(4,4′-dimethoxytrityloxy)ethyl]-3-(uracil-1-yl)-2,5-dioxabicyclo[2.2.1]heptane (28). 28 was prepared according to the general procedure, using **26** (0.18 g, 0.31 mmol) to provide **28** (0.2 g, 81%). ^{31}P NMR (121 MHz, $CDCl_3$) δ: 149.4, 148.6.

Acknowledgment. We thank Dr. Karsten Schmidt for HRMS measurements.

Supporting Information Available: General experimental procedures for synthesis of **29**, **30**, **31**, and *R*- and *S*-5′-Me-LNA cytosine phosphoramidites; ^{1}H and ^{13}C NMR spectra for all new compounds; ^{31}P NMR spectra for phosphoramidites; analytical data for oligonucleotides. This material is available free of charge via the Internet at http://pubs.acs.org.

References

(1) Bennett, C. F.; Swayze, E. E. RNA targeting therapeutics: molecular mechanisms of antisense oligonucleotides as a therapeutic platform. *Annu. Rev. Pharmacol. Toxicol.* **2010**, *50*, 259–293.
(2) Swayze, E. E.; Bhat, B. The Medicinal Chemistry of Oligonucleotides. In *Antisense Drug Technology: Principles, Strategies, and Applications*, 2nd ed.; Crooke, S. T., Ed.; CRC Press: Boca Raton, FL, 2008; pp 143−182.
(3) De Paula, D.; Bentley, M. V.; Mahato, R. I. Hydrophobization and bioconjugation for enhanced siRNA delivery and targeting. *RNA* **2007**, *13*, 431–456.
(4) Semple, S. C.; Akinc, A.; Chen, J.; Sandhu, A. P.; Mui, B. L.; Cho, C. K.; Sah, D. W.; Stebbing, D.; Crosley, E. J.; Yaworski, E.; Hafez, I. M.; Dorkin, J. R.; Qin, J.; Lam, K.; Rajeev, K. G.; Wong, K. F.; Jeffs, L. B.; Nechev, L.; Eisenhardt, M. L.; Jayaraman, M.; Kazem, M.; Maier, M. A.; Srinivasulu, M.; Weinstein, M. J.; Chen, Q.; Alvarez, R.; Barros, S. A.; De, S.; Klimuk, S. K.; Borland, T.; Kosovrasti, V.; Cantley, W. L.; Tam, Y. K.; Manoharan, M.; Ciufolini, M. A.; Tracy, M. A.; de Fougerolles, A.; MacLachlan, I.; Cullis, P. R.; Madden, T. D.; Hope, M. J. Rational design of cationic lipids for siRNA delivery. *Nat. Biotechnol.* **2010**, *28*, 172–176.
(5) Bennett, C. F.; Swayze, E.; Geary, R.; Henry, S.; Tillman, L.; Hardee, G. Antisense Oligonucleotide-Based Therapeutics. In *Gene and Cell Therapy: Therapeutic Mechanisms and Strategies*, 3rd ed.; Smyth Templeton, N., Ed.; CRC Press: Boca Raton, FL, 2009; pp 497−522.
(6) Raal, F. J.; Santos, R. D.; Blom, D. J.; Marais, A. D.; Charng, M. J.; Cromwell, W. C.; Lachmann, R. H.; Gaudet, D.; Tan, J. L.; Chasan-Taber, S.; Tribble, D. L.; Flaim, J. D.; Crooke, S. T. Mipomersen, an apolipoprotein B synthesis inhibitor, for lowering of LDL cholesterol concentrations in patients with homozygous familial hypercholesterolaemia: a randomised, double-blind, placebo-controlled trial. *Lancet* **2010**, *375*, 998–1006.
(7) Geary, R. S.; Yu, R. Z.; Levin, A. A. Pharmacokinetics of phosphorothioate antisense oligodeoxynucleotides. *Curr. Opin. Invest. Drugs* **2001**, *2*, 562–573.
(8) Geary, R. S. Antisense oligonucleotide pharmacokinetics and metabolism. *Expert Opin. Drug Metab. Toxicol.* **2009**, *5*, 381–391.
(9) Prakash, T. P.; Bhat, B. 2′-Modified oligonucleotides for antisense therapeutics. *Curr. Top. Med. Chem.* **2007**, *7*, 641–649.
(10) Martin, P. Ein neuer zugang zu 2-*O*-alkylribonucleosiden und eigenschaften deren oligonucleotide. *Helv. Chim. Acta* **1995**, *78*, 486–504.
(11) Teplova, M.; Minasov, G.; Tereshko, V.; Inamati, G. B.; Cook, P. D.; Manoharan, M.; Egli, M. Crystal structure and improved antisense properties of 2′-*O*-(2-methoxyethyl)-RNA. *Nat. Struct. Biol.* **1999**, *6*, 535–539.
(12) Wengel, J. Synthesis of 3′-*C*- and 4′-*C*-branched oligodeoxynucleotides and the development of locked nucleic acid (LNA). *Acc. Chem. Res.* **1999**, *32*, 301–310.

(13) Imanishi, T.; Obika, S. BNAs: novel nucleic acid analogs with a bridged sugar moiety. *Chem. Commun.* **2002**, 1653–1659.
(14) Lanford, R. E.; Hildebrandt-Eriksen, E. S.; Petri, A.; Persson, R.; Lindow, M.; Munk, M. E.; Kauppinen, S.; Orum, H. Therapeutic silencing of microRNA-122 in primates with chronic hepatitis C virus infection. *Science* **2010**, *327*, 198–201.
(15) Straarup, E. M.; Fisker, N.; Hedtjarn, M.; Lindholm, M. W.; Rosenbohm, C.; Aarup, V.; Hansen, H. F.; Orum, H.; Hansen, J. B.; Koch, T. Short locked nucleic acid antisense oligonucleotides potently reduce apolipoprotein B mRNA and serum cholesterol in mice and non-human primates. *Nucleic Acids Res.* [Online early access]. DOI: 10.1093/nar/gkq457 Published Online: July 8, 2010.
(16) Gupta, N.; Fisker, N.; Asselin, M. C.; Lindholm, M.; Rosenbohm, C.; Orum, H.; Elmen, J.; Seidah, N. G.; Straarup, E. M. A locked nucleic acid antisense oligonucleotide (LNA) silences PCSK9 and enhances LDLR expression in vitro and in vivo. *PLoS One* **2010**, *5*, No. e10682.
(17) Graziewicz, M. A.; Tarrant, T. K.; Buckley, B.; Roberts, J.; Fulton, L.; Hansen, H.; Orum, H.; Kole, R.; Sazani, P. An endogenous TNF-alpha antagonist induced by splice-switching oligonucleotides reduces inflammation in hepatitis and arthritis mouse models. *Mol. Ther.* **2008**, *16*, 1316–1322.
(18) Swayze, E. E.; Siwkowski, A. M.; Wancewicz, E. V.; Migawa, M. T.; Wyrzykiewicz, T. K.; Hung, G.; Monia, B. P.; Bennett, C. F. Antisense oligonucleotides containing locked nucleic acid improve potency but cause significant hepatotoxicity in animals. *Nucleic Acids Res.* **2007**, *35*, 687–700.
(19) Seth, P. P.; Siwkowski, A.; Allerson, C. R.; Vasquez, G.; Lee, S.; Prakash, T. P.; Kinberger, G.; Migawa, M. T.; Gaus, H.; Bhat, B.; Swayze, E. E. Design, synthesis and evaluation of constrained methoxyethyl (cMOE) and constrained ethyl (cEt) nucleoside analogs. *Nucleic Acids Symp. Ser.* **2008**, 553–554.
(20) Seth, P. P.; Siwkowski, A.; Allerson, C. R.; Vasquez, G.; Lee, S.; Prakash, T. P.; Wancewicz, E. V.; Witchell, D.; Swayze, E. E. Short antisense oligonucleotides with novel 2′-4′ conformationaly restricted nucleoside analogues show improved potency without increased toxicity in animals. *J. Med. Chem.* **2009**, *52*, 10–13.
(21) Seth, P. P.; Vasquez, G.; Allerson, C. A.; Berdeja, A.; Gaus, H.; Kinberger, G. A.; Prakash, T. P.; Migawa, M. T.; Bhat, B.; Swayze, E. E. Synthesis and biophysical evaluation of 2′,4′-constrained 2′O-methoxyethyl and 2′,4′-constrained 2′O-ethyl nucleic acid analogues. *J. Org. Chem.* **2010**, *75*, 1569–1581.
(22) Srivastava, P.; Barman, J.; Pathmasiri, W.; Plashkevych, O.; Wenska, M. g.; Chattopadhyaya, J. Five- and six-membered conformationally locked 2′,4′-carbocyclic *ribo*-thymidines: synthesis, structure, and biochemical studies. *J. Am. Chem. Soc.* **2007**, *129*, 8362–8379.
(23) Seth, P. P.; Allerson, C. R.; Berdeja, A.; Siwkowski, A.; Pallan, P. S.; Gaus, H.; Prakash, T. P.; Watt, A. T.; Egli, M.; Swayze, E. E. An exocyclic methylene group acts as a bioisostere of the 2′-oxygen atom in LNA. *J. Am. Chem. Soc.* **2010**, *132*, 14942–14950.
(24) Prakash, T. P.; Siwkowski, A.; Allerson, C. R.; Migawa, M. T.; Lee, S.; Gaus, H. J.; Black, C.; Seth, P. P.; Swayze, E. E.; Bhat, B. Antisense oligonucleotides containing conformationally constrained 2′,4′-(*N*-methoxy)aminomethylene and 2′,4′-aminooxymethylene and 2′-*O*,4′-*C*-aminomethylene bridged nucleoside analogues show improved potency in animal models. *J. Med. Chem.* **2010**, *53*, 1636–1650.
(25) Saha, A. K.; Caulfield, T. J.; Hobbs, C.; Upson, D. A.; Waychunas, C.; Yawman, A. M. 5′-Me-DNA. A new oligonucleotide analog: synthesis and biochemical properties. *J. Org. Chem.* **1995**, *60*, 788–789.
(26) Wang, G.; Middleton, P. J. 5′-C-branched thymidines: synthesis, stereochemistry, and incorporation into oligodeoxynucleotides. *Tetrahedron Lett.* **1996**, *37*, 2739–2742.
(27) De Mesmaeker, A.; Lebreton, J.; Jouanno, C.; Fritsch, V.; Wolf, R. M.; Wendeborn, S. Amide-modified oligonucleotides with preorganized backbone and furanose rings: highly increased thermodynamic stability of the duplexes formed with their RNA and DNA complements. *Synlett* **1997**, 1287–1290.
(28) Leumann, C. J. DNA analogues: from supramolecular principles to biological properties. *Bioorg. Med. Chem.* **2002**, *10*, 841–854.
(29) Dupouy, C.; Iche-Tarrat, N.; Durrieu, M. P.; Rodriguez, F.; Escudier, J. M.; Vigroux, A. Watson−Crick base-pairing properties of nucleic acid analogues with stereocontrolled alpha and beta torsion angles (alpha,beta-D-CNAs). *Angew. Chem., Int. Ed.* **2006**, *45*, 3623–3627.
(30) Dupouy, C.; Iche-Tarrat, N.; Durrieu, M. P.; Vigroux, A.; Escudier, J. M. Alpha,beta-D-CNA induced rigidity within oligonucleotides. *Org. Biomol. Chem.* **2008**, *6*, 2849–2851.
(31) Sharma, P. K.; Mikkelsen, B. H.; Christensen, M. S.; Nielsen, K. E.; Kirchhoff, C.; Pedersen, S. L.; Sorensen, A. M.; Ostergaard, K.; Petersen, M.; Nielsen, P. A cyclic dinucleotide with a four-carbon 5′-C-to-5′-C connection; synthesis by RCM, NMR-examination and incorporation into secondary nucleic acid structures. *Org. Biomol. Chem.* **2006**, *4*, 2433–2445.
(32) Wu, X.; Pitsch, S. Synthesis and pairing properties of oligoribonucleotide analogues containing a metal-binding site attached to β-D-allofuranosyl cytosine. *Nucleic Acids Res.* **1998**, *26*, 4315–4323.
(33) Wang, J.; Verbeure, B.; Luyten, I.; Lescrinier, E.; Froeyen, M.; Hendrix, C.; Rosemeyer, H.; Seela, F.; Van Aerschot, A.; Herdewijn, P. Cyclohexene nucleic acids (CeNA): serum stable oligonucleotides that activate RNase H and increase duplex stability with complementary RNA. *J. Am. Chem. Soc.* **2000**, *122*, 8595–8602.
(34) Kvaerno, L.; Wengel, J. Antisense molecules and furanose conformations—is it really that simple? *Chem. Commun.* **2001**, 1419–1424.
(35) Kvrno, L.; Kumar, R.; Dahl, B. M.; Olsen, C. E.; Wengel, J. Synthesis of abasic locked nucleic acid and two seco-LNA derivatives and evaluation of their hybridization properties compared with their more flexible DNA counterparts. *J. Org. Chem.* **2000**, *65*, 5167–5176.
(36) Bondensgaard, K.; Petersen, M.; Singh, S. K.; Rajwanshi, V. K.; Kumar, R.; Wengel, J.; Jacobsen, J. P. Structural studies of LNA: RNA duplexes by NMR: conformations and implications for RNase H activity. *Chem.—Eur. J.* **2000**, *6*, 2687–2695.
(37) Nielsen, K. E.; Singh, S. K.; Wengel, J.; Jacobsen, J. P. Solution structure of an LNA hybridized to DNA: NMR study of the d(CTLGCTLTLCTLGC):d(GCAGAAGCAG) duplex containing four locked nucleotides. *Bioconj. Chem.* **2000**, *11*, 228–238.
(38) Petersen, M.; Bondensgaard, K.; Wengel, J.; Jacobsen, J. P. Locked nucleic acid (LNA) recognition of RNA: NMR solution structures of LNA:RNA hybrids. *J. Am. Chem. Soc.* **2002**, *124*, 5974–5982.
(39) Kaur, H.; Arora, A.; Wengel, J.; Maiti, S. Thermodynamic, counterion, and hydration effects for the incorporation of locked nucleic acid nucleotides into DNA duplexes. *Biochemistry* **2006**, *45*, 7347–7355.
(40) Egli, M.; Teplova, M.; Minasov, G.; Kumar, R.; Wengel, J. X-ray crystal structure of a locked nucleic acid (LNA) duplex composed of a palindromic 10-mer DNA strand containing one LNA thymine monomer. *Chem. Commun* **2001**, 651–652.
(41) Saenger, W. *Principles of Nucleic Acid Structure.*; Springer-Verlag: New York, 1984; pp 1−556.
(42) Rubin, J.; Brennan, T.; Sundaralingam, M. Crystal and molecular structure of a naturally occurring dinucleoside monophosphate. Uridylyl-(3′-5′)-adenosine hemihydrate. Conformational rigidity of the nucleotide unit and models for polynucleotide chain folding. *Biochemistry* **1972**, *11*, 3112–3128.
(43) Portmann, S.; Usman, N.; Egli, M. The Crystal structure of r(CCCCGGGG) in two distinct lattices. *Biochemistry* **1995**, *34*, 7569–7575.
(44) Egli, M.; Lubini, P.; Bolli, M.; Dobler, M.; Leumann, C. Crystal structure of a parallel-stranded duplex of a deoxycytidylyl-(3′-5′)-deoxycytidine analog containing intranucleosidyl C(3′)−C(5′) ethylene bridges. *J. Am. Chem. Soc.* **1993**, *115*, 5855–5856.
(45) Tarkov, M.; Bolli, M.; Schweizer, B.; Leumann, C. Nucleic-acid analogs with constraint conformational flexibility in the sugar-phosphate backbone ("bicyclo-DNA"). Part 1. Preparation of (3′*S*,5′*R*)-2′-deoxy-3′,5′-ethano-ab-D-ribonucleosides (bicyclonucleosides). *Helv. Chim. Acta* **1993**, *76*, 481–510.
(46) Pallan, P. S.; Ittig, D.; Heroux, A.; Wawrzak, Z.; Leumann, C. J.; Egli, M. Crystal structure of tricyclo-DNA: an unusual compensatory change of two adjacent backbone torsion angles. *Chem. Commun.* **2008**, 883–885.
(47) Freier, S. M.; Altmann, K. H. The ups and downs of nucleic acid duplex stability: structure−stability studies on chemically-modified DNA:RNA duplexes. *Nucleic Acids Res.* **1997**, *25*, 4429–4443.